Pharm Res (2015) 32:1354–1367
DOI 10.1007/s11095-014-1539-4

RESEARCH PAPER

Short-Chain Glycoceramides Promote Intracellular Mitoxantrone Delivery from Novel Nanoliposomes into Breast Cancer Cells

Lília R. Cordeiro Pedrosa • Timo L. M. ten Hagen • Regine Süss • Albert van Hell • Alexander M. M. Eggermont • Marcel Verheij • Gerben A. Koning

Received: 24 April 2014 / Accepted: 29 September 2014 / Published online: 16 October 2014

ABSTRACT

Purpose To improve therapeutic activity of mitoxantrone (MTO)-based chemotherapy by reducing toxicity through encapsulation in nanoliposomes and enhancing intracellular drug delivery using short-chain sphingolipid (SCS) mediated tumor cell membrane permeabilization.

Methods Standard (MTOL) and nanoliposomes enriched with the SCS, C8-Glucosylceramide or C8-Galactosylceramide (SCS-MTOL) were loaded by a transmembrane ammonium sulphate gradient and characterized by DLS and cryo-TEM. Intracellular MTO delivery was measured by flow cytometry and imaged by fluorescence microscopy. In vitro cytotoxicity was studied in breast carcinoma cell lines. Additionally, live cell confocal microscopy addressed the drug delivery mechanism by following the intracellular fate of the nanoliposomes, the SCS and MTO. Intratumoral MTO localization in relation to CD31-positive tumor vessels and CD11b positive cells was studied in an orthotopic MCF-7 breast cancer xenograft.

Results Stable SCS-MTOL were developed increasing MTO delivery and cytotoxicity to tumor cells compared to standard MTOL. This effect was much less pronounced in normal cells. The drug delivery mechanism involved a transfer of SCS to the cell membrane, independently of drug transfer and not involving nanoliposome internalization. MTO was detected intratumorally upon MTOL and SCS-MTOL treatment, but not after free MTO, suggesting an important improvement in tumor drug delivery by nanoliposomal formulation. Nanoliposomal MTO delivery and cellular uptake was heterogeneous throughout the tumor and clearly correlated with CD31-positive tumor vessels. Yet, MTO uptake by CD11b positive cells in tumor stroma was minor.

Conclusions Nanoliposomal encapsulation improves intratumoral MTO delivery over free drug. Liposome bilayer-incorporated SCS preferentially permeabilize tumor cell membranes enhancing intracellular MTO delivery.

KEY WORDS Mitoxantrone · Chemotherapy · Short-chain sphingolipids · Tumor-cell membrane-permeability modulation · Targeting tumor cell membrane

Electronic supplementary material The online version of this article (doi:10.1007/s11095-014-1539-4) contains supplementary material, which is available to authorized users.

L. R. C. Pedrosa • T. L. M. ten Hagen • A. M. M. Eggermont • G. A. Koning (✉)
Section Surgical Oncology, Department of Surgery Laboratory Experimental Surgical Oncology, Room Ee151b, Erasmus MC 3000CA RotterdamPO Box 2040, The Netherlands
e-mail: g.koning@erasmusmc.nl

R. Süss
Department of Pharmaceutical Technology and Biopharmacy Albert-Ludwigs University, D-79104 Freiburg, Germany

A. van Hell • M. Verheij
Division of Biological Stress Response he Netherlands Cancer Institute - Antoni van Leeuwenhoek Hospital, Amsterdam 1066 CX, The Netherlands

A. M. M. Eggermont
Institut de Cancerologie Gustave Roussy, Villejuif Paris 94800, France

M. Verheij
Department of Radiotherapy The Netherlands Cancer Institute - Antoni van Leeuwenhoek Hospital, Amsterdam 1066 CX, The Netherlands

INTRODUCTION

Mitoxantrone (MTO) is an anthracenedione, a group of synthetic chemotherapeutic drugs. It is the most potent of many ametantrone derivatives that were identified in a quest for synthetic anthracyclin-related compounds with potential chemotherapeutic activity [1, 2]. Due to their chemical similarity to the naturally occurring antitumor antibiotics, such as the anthracyclines doxorubicin and daunorubicin and related drugs such as bleomycin and mitomycin-C, MTO exerts similar mechanisms of action and antitumor activities. However, lower cardiotoxicity as side effects has been described for MTO [3–5].

MTO has gained importance in the treatment of metastatic breast cancer over the use of anthracyclines [6, 7] due to its similar therapeutic activity, which is exerted with less severe gastrointestinal toxicity, cardiotoxicity and alopecia at equally myelosuppressive doses [8]. Numerous studies on the mechanism of action of MTO indicate that nuclear DNA is the major target for this drug [9–12]. Binding of MTO to DNA causes DNA condensation, inhibits replication and RNA transcription. MTO is also a potent inhibitor of topoisomerase II, an enzyme involved in control of DNA topology through breaking and rejoining double-stranded DNA [2, 3]. More recently it was proven that MTO binds to chromatin and produces a compact structure, a finding which is in good agreement with the inhibitory effects on DNA replication and RNA transcription [12, 13]. Despite the improved toxicity profile of MTO compared to anthracyclines, significant side effects still remain [6, 7].

It is well established that the therapeutic index of anticancer agents can be improved through application of liposomal drug carrier technology [14]. Encapsulation in liposomes may reduce toxic side effects and increase drug levels in tumors [15–17]. Liposomes are rationally designed to entrap drugs while in circulation, thereby reducing the exposure of healthy tissue and selectively delivering them locally in the tumor by virtue of the enhanced permeability and retention effect [17]. Sterically stabilized liposomes exhibit extended blood circulation time, which together with their small size of <100 nm can result in tumor accumulation [17, 18]. However the slow drug release, the presence of the tumor cell membrane barrier and thus limited intracellular drug bioavailability after liposome accumulation in the tumor, represent important factors limiting efficacy of liposomal chemotherapy [19–23].

Previously, we reported that short chain sphingolipids (SCS), like C_8-glucosylceramide (C_8-GluCer) or C_8-galactosylceramide (C_8-GalCer) can significantly potentiate intracellular drug uptake of free or liposome-encapsulated drugs and thereby enhance their efficacy, [24–28]. It is hypothesized, that a dynamic biophysical mechanism is responsible for the enhanced drug delivery properties of SCS upon their insertion into the tumor cell membrane [27, 28]. The modulation of tumor cell membrane lipid composition by SCS may result in specific pore domains in the cell membrane, increasing cellular drug influx [28, 29]. In the current study we broaden the application of this novel drug delivery strategy targeting the plasma membrane lipid composition to MTO. The aim is to develop novel effective liposomal MTO formulations, which benefit from reduction in toxicity through liposomal encapsulation and the SCS-mediated cellular drug uptake enhancement. We therefore co-formulated both SCS and MTO in the same lipid nanovehicle for co-delivery to tumor cells thereby improving therapeutic activity of MTO based chemotherapy.

Here we developed an optimal loading method for liposomal MTO with high drug loading efficiency and stability. Next, we investigated intracellular drug delivery using these SCS-enriched liposomal MTO in comparison to non-enriched liposomal MTO and finally addressed intratumoral MTO localization in a breast carcinoma model.

MATERIAL AND METHODS

Materials & Reagents

Hydrogenated soy phosphatidylcholine (HSPC) and distearylphosphatidylethanolamine (DSPE)-PEG_{2000} were from Lipoid (Ludwigshaven, Germany). Short chain sphingolipids, C_8 Glucosyl(ß) Ceramide (d18:1/8:0) D-glucosyl-ß-1,1′ N-octanoyl-D-erythro-sphingosine (C_8-GluCer), C_8 Galactosyl(ß) Ceramide (d18:1/8:0) D-galactosyl-ß-1,1′ N-octanoyl-D-erythro-sphingosine (C_8-GalCer), C_6-NBD Galactosyl Ceramide N-[6-[(7-nitro-2-1,3-benzoxadiazol-4-yl)amino]hexanoyl]-D-galactosyl-ß1-1′-sphingosine and 16:0 Liss Rhod PE 1,2-dipalmitoyl-sn-glycero-3-phosphoethanolamine-N-(lissamine rhodamine B sulfonyl) (ammonium salt) were from Avanti Polar Lipids (Alabaster, AL, USA).

Polycarbonate filters were from Northern Lipids (Vancouver, BC, Canada) and PD-10 Sephadex columns were from GE Healthcare (Diegem, Belgium). Cholesterol, HEPES (2-[4-(2-hydroxyethyl)piperazin-1-yl] ethanesulfonic acid), trichloroacetic acid (TCA) , acetic acid, Triton-X, sulforhodamine B (SRB) were from Sigma Aldrich (Zwijndrecht, The Netherlands). DAPI nuclear dye, diamidino-2-phenylindole was from Molecular Probes (Leiden, The Netherlands). PBS was from Boom and FACS flow fluid from BD Biosciences. Mitoxantrone dihydrocchloride, 2 mg*ml^{-1} (OnKotrone) was from Baxter.

Liposome Formulation

Liposomes were formulated of HSPC/ Cholesterol/ DSPE-PEG_{2000} in a molar ratio of 1.85: 1: 0.15. To the mixture of lipids 0.1 mol of SCS was added per mole of total amount of lipid (including cholesterol).

Liposomes of 85–100 nm in diameter were prepared by lipid film hydration and extrusion method using a thermobarrel extruder, Northern Lipids, Vancouver, Canada at 65°C [30].

Lipids were dissolved in chloroform methanol (9:1 *v/v*), mixed and a lipid film was created under reduced pressure on a rotary evaporator and subsequently dried under a stream of nitrogen. To optimize drug loading efficiency different loading methods were tested in parallel to different drug to phospholipid ratios (D:PL) (*w/w*) as described in literature for

MTO liposomal loading [31–33]. A transmembrane pH gradient driven loading procedure was tested at a D:PL ratio of 0.08 (*w*/*w*) at 65°C as described by Lim et al. [33]. Additional drug loading methods were based on ammonium sulfate gradient method [30] at 65°C considering different D:PL loading ratios (*w*/*w*) of 0.08 and 0.036 [31, 32]. Finally, lipid film was hydrated by addition of 250 mM of $(NH_4)_2SO_4$, pH 5.5 and liposomes were sized by sequential extrusion through 100-, 80-, and 50 nm polycarbonate filters (Northern Lipids, Vancouver, Canada). Non encapsulated $(NH_4)_2SO_4$ was removed by gel filtration chromatography using PD-10 Sephadex column (GE Healthcare, Diegem, Belgium), eluted with 135 mM NaCl, 10 mM Hepes buffer, pH 7.4.

Empty liposomes were heated at 65°C for 10 min and MTO was added to liposomes in each respective drug to D:PL (*w*/*w*). After loading and separation of free from entrapped liposomal drug, size and polydispersity index (pdi) were determined by light scattering using a Zetasizer Nano ZS (Malvern Instruments, Malvern, UK). Lipid concentration was measured by phosphate assay [34].

After separation of free non-encapsulated MTO from liposome-encapsulated MTO, the amount of entrapped drug was measured by fluorimetry ($\lambda_{exCitation}$ 607 nm; $\lambda_{emission}$ 684 nm) and measured after entire liposome solubilization with 1% (*v*/*v*) Triton in water to a calibration curve from stock MTO, 2 mg*ml^{-1}. Loading efficiency was calculated as a percentage of recovered amounts of drug entrapped in the liposome, in relation to the initial amount of drug added for loading.

Fluorescent labelled liposomes and fluorescent labelled SCS liposomes were prepared using fluorescent lipid Rhodamine and C6-NBD Galactosyl Ceramide, respectively, at 0.1% and 0.25 mol% of total amount of lipid.

Stability

Long-Term Storage Conditions

Long-term storage conditions stability at 4°C was based on size, pdi and MTO content measurements for a period of at least 1 year. All measurements were performed in triplicate. MTO content was measured as reported in previous section after separation of free drug by gel filtration chromatography.

Short-Term Storage Conditions, 37°C

Stability studies of non-enriched (standard) and SCS-enriched-MTO liposomal formulations were performed for 24 h at 37°C, in the absence and presence of 10 or 50% human serum. MTO release was quantified as described in previous section. Total drug release was measured after entire liposomal solubilization by adding 1% (*v*/*v*) of Triton-X in water and human serum as blank was subtracted from sample release and total release measurements. Values were presented as percentage of liposomal drug content and calculated following the formula:

$$\%\ Entrapped\ MTO = 100 - \left[\left(Fluorescence_{sample} - blank\right) * 100 / \left(Fluorescence_{total\ release} - blank\right)\right]$$

Cryo-Transmission Electron Microscopy (TEM)

Cryo-TEM was used to characterize the detailed structure of the liposomal formulations (non-enriched, C_8-GluCer and C_8-GalCer-MTOL) of MTO and the physical state of the encapsulated drug. The freezing was performed in a cooling chamber which was permanently cooled with liquid nitrogen. A sample droplet was placed on a microperforated copper grid and blotted by a filter paper to result in a thin liquid film. The grid was plunged into liquid ethane for immediate freezing. A Leo 912 Omega TEM microscope (Carl Zeiss NTS GmbH, Oberkochen, Germany) was used.

Cell Culture

All tumor cell lines were cultured in Dulbeccos's modified Eagle medium, supplemented with 10% fetal calf serum and 4 mM L-glutamine. HUVEC were isolated by collagenase digestion using the method described by Jaffe *et al.* [35] and cultured in HUVEC medium containing human endothelial serum free medium (Invitrogen), 20% heat inactivated newborn calf serum (Cambrex), 10% heat inactivated human serum (Cambrex), 20 ng/ml human recombinant epidermal basic fibroblast growth factor (Peprotech EC Ltd) and 100 ng/ml human recombinant epidermal growth factor (Peprotech EC Ltd) in fibronectin (Roche Diagnostics) coated flasks. Fibroblasts (3T3) were purchased from Biowhitakker and cultured in Dulbeccos's modified Eagle medium containing nutrient mixture F12, supplemented with 10% fetal calf serum and 4 mM L-glutamine.

In vitro Drug Efficacy

Human breast carcinoma cells, MCF-7 and SKBR3 (1.25×10^4 cells/ well) were plated in flat bottom 96 well plates. After 24 h at 37°C, cells were exposed to serial concentrations of

MTO-liposomal formulations and free MTO in culture medium for 24 h.

Cell survival was determined by measuring total cellular protein levels using the sulforhodamine-B (SRB) assay [36]. Cells were washed twice with PBS, incubated with 10% trichloric acetic acid (1 h, 4°C) and washed again. Cells were stained with 0.4% SRB (Sigma) for 15 min and washed with 1% acetic acid. After drying, protein-bound SRB was dissolved in TRIS buffer (10 mM, pH 9.4) and absorbance was measured at a wavelength of 540 nm in a plate reader. Cell survival was calculated as a percentage relative to control (untreated cells), which was set at 100%.

$IC_{50,}$ the concentration that inhibits 50% of cellular growth, was determined for each MTO liposomal formulation, by plotting the cell survival observed for each concentration versus the log concentration and non-linear regression curve fitting using GraphPad Prism software v5.0. In all experiments incubations were performed in triplicate at least with three different batches.

Intracellular MTO Delivery Measured by Flow Cytometry

Cells were seeded on flat bottom 24 well plates at a final concentration of 6×10^4 cells/ well and allowed to adhere for 24 h. Non-enriched and SCS-MTOL, diluted in growth medium were added resulting in a final drug concentration of 10 μM, and incubated for 4 and 24 h. After incubation, cells were washed twice to discard non-incorporated drug and trypsinized for 2 min. Cell suspensions were washed twice in medium and resuspended in PBS. Cellular fluorescence representing drug uptake was analyzed with a Becton Dickinson FACScan using Cell Quest software by the fluorescent signal detected in the FL4 channel after excitation at 635 nm. Per analysis 10,000 cells were counted.

Intracellular Fate of SCS and Drug

Fluorescently labelled NBD-C_6-GalCer-MTOL were added to SKBR-3 breast carcinoma cells (1×10^5 cells) in 10% serum medium and incubated for 2 h at 37°C. A Zeiss LSM Meta confocal microscope was used for live cell imaging with 488 nm excitation and BP 505–530 nm emission for the SCS and 543 nm excitation and BP 550–615 nm emission for Rhodamine labelled liposomes. MTO was imaged at 633 nm excitation and LP 650 nm emission, with a 63× plan apo (na 1.4) oil lens.

Intratumoral MTO Delivery

MTO delivery and intratumoral fate was evaluated 24 h after a single i.v administration of MTO, 5 mg*Kg^{-1} in form of MTO and C_8-GluCer or C_8-GalCer-MTOL in a MCF-7 breast carcinoma tumor model, implanted orthotopically [37]. Tumors with a diameter of 8 to 10 mm were excised, immediately snap-frozen in liquid nitrogen and stored at −80°C until further analysis. The endothelial cells of blood vessels and tissue macrophages were stained immunohistochemically, using the same frozen sections as for MTO imaging. As during sample preparation, fixation and staining, MTO fluorescence will be partly lost, cryosections before staining were used for measuring MTO fluorescence intensity without further contact of the sections with solvents. After MTO imaging, cryostat sections of 5 μm were air dried and fixed with acetone for 5 min. After Tris Buffer Saline (TBS) washing and blocking step with 10% Normal Goat Serum (ABD Serotec) in 1%BSA (Sigma) for 10 min, sections were incubated with primary antibody, rat anti mouse monoclonal CD31(BD Pharmingen) for endothelial cells of blood vessels staining, in 1%BSA for 1 h at room temperature. Thereafter, sections were washed with TBS and incubated for 30 min with goat anti rabbit Alexa Fluor 488 secondary antibody (In vitrogen) in 1%BSA/PBS. For macrophages staining, after Tris Buffer Saline (TBS) washing and blocking, step sections were incubated with primary antibody, rat anti mouse monoclonal anti-CD11b (eBioscience) in 1%BSA for 1 h at room temperature. After washing, sections were incubated with goat anti rabbit Alexa Fluor 488 secondary antibody (Invitrogen) in 1%BSA/PBS for 30 min. After washing, sections were covered with DAPI 1:1000 for nuclear staining. Imaging was performed with a Leica SP5 microscope for MTO at 633 nm 670 LP, previously to staining.

Statistics

Statistical analysis was performed using the ANOVA test. P-values less than 0.05 were considered statistically significant. All parametric values are expressed as mean ± standard error of the mean (SEM). Calculations were performed using GraphPad Prism v5.0.

RESULTS

Formulation of Glycoceramide-MTO Nanoliposomes

Non-enriched-MTOL (standard MTOL) and SCS-MTOL formulations were prepared using two different buffers to hydrate the lipid film to create a gradient for subsequent drug loading and different lipid:PL ratios. Liposomes prepared in citrate buffer presented size <100 nm and pdi < 0.1, but when loaded with MTO in a D:PL (*w*/*w*) of 0.08 [33] the loading efficiency was <10% (Supplemental table 1) and preparations displayed visible liposomal aggregation for non-enriched and SCS-MTOL (data not shown). When ammonium sulfate loading was used, MTO loading efficiency increased to 70%

[31, 32] (Supplemental Table 1) and no particle aggregation was observed (data not shown). MTOL loaded by ammonium sulfate gradient method at a final D:PL (*w*/*w*) of 0.07 resulted in maximal MTO drug loading of 100% for SCS-MTOL whereas MTOL had 75% MTO entrapped. These optimized formulations had a size of around 85 nm in diameter with a high level of homogeneity indicated by a pdi < 0.1 (Table I), regardless of the presence or absence of C_8-GalCer or C_8-GluCer and were used for further experiments. No lipid loss from nanoparticles was observed during loading procedure.

MTO is Retained in SCS Enriched-MTOL

Long-Term Storage Conditions

C_8-GluCer or C_8-GalCer-MTOL showed a stability profile similar to MTOL. Weekly assessment of particle size, pdi and entrapped drug levels revealed 6–19%MTO release from liposomes, which occurred in the first week of storage. After this initial release which was equal between MTOL and C_8-GalCer-MTOL, but lower for C_8-GluCer-MTOL, liposomes retained their drug contents up to 1 year. Particle size and pdi remained constant up to 1 year at 4°C (Fig. 1 and Table I).

Stability Under In Vitro Cell Culture and In Vivo Conditions

Under cell culture conditions at 37°C in the absence and presence of 10% of serum, or upon the presence of 50% human serum in Hepes buffer at 37°C, C_8-GluCer and C_8-GalCer–MTOL efficiently retained high levels of their drug contents up to 24 h (Fig. 2). In the absence of serum at 37°C, SCS-MTOL and MTOL retained 100% of their drug content (Fig. 2a). In 10% of human serum at 37°C, both SCS-MTOL displayed initial drug release of 10–15% in the first hour (Fig 2b, insert) and a more gradual release of another 5–10% up to 24 h, similar to MTOL (Fig. 2b). When exposed to 50% human serum at 37°C, mimicking the conditions in blood circulation, SCS-MTOL showed an initial release of around 20% of drug (Fig 2c, insert), followed by a phase with minimal release up to 24 h. Non-enriched-MTOL showed a more gradual and continuous drug release of 25–30% during 24 h (Fig. 2c).

Morphology of Nanoliposomes Containing MTO by Cryo-Transmission Electron Microscopy

Cryogenic transmission electron microscopy (cryo-TEM) analysis of MTOL formulations demonstrated an intraliposomal crystallized gel-like form of MTO visible in the hydrophilic core of all formulations (Fig. 3). All three liposomal formulations presented a homogeneous population of uniformly round-shaped vesicles with sizes confirming DLS measurements.

In Vitro Liposomal MTO Efficacy is Enhanced by SCS

In vitro efficacy of liposomal MTO formulations was tested towards human MCF-7 and SKBR3, breast carcinoma cell lines. In both cell lines, C_8-GluCer and C_8-GalCer-MTOL exerted increased cytotoxicity compared to non-enriched MTOL after a 24 h incubation time at 37°C (Fig. 4). At concentrations of 10 μM and higher, SCS-MTOL had significantly higher anti-tumor activity than MTOL ($p<0.05$). IC_{50} values of both SCS-enriched formulations were over 100-fold lower than non-enriched MTOL and approached IC_{50} concentrations achieved for free MTO in SKBR3 and MCF-7 carcinoma cells (Table II).

Breast Carcinoma Cells Demonstrate Higher Sensitivity to C_8-GalCer Mediated MTO Uptake

MTO uptake was measured by flow cytometry in SKBR-3 breast carcinoma cells and compared to human endothelial cells (HUVEC) and fibroblasts (3T3). Cells were treated with non-enriched MTOL, C_8-GluCer or C_8-GalCer–MTOL for 4 or 24 h at a concentration of 10 μM MTO. The presence of C_8-GluCer or C_8-GalCer in the liposomal bilayer enhanced intracellular drug uptake in SKBR-3 tumor cells at both time points (Fig. 5). Remarkably, C_8-GalCer increased intracellular drug levels 12–15 fold compared to non-enriched liposomes ($p<0.001$), whereas C_8-GluCer enhanced drug uptake 3 fold, but not significantly in relation to non-enriched liposomes ($p>0.05$). The increased drug levels observed in SKBR-3 cells treated with C_8-GalCer-MTOL correspond to the *in vitro* cytotoxicity data (Fig. 4).

Table I Characterization of optimized MTO-nanoliposomes

MTOL	D:PL($^w/_w$)$_{initial}$	D:PL($^w/_w$)$_{extrusion}$ ± SEM	D:PL($^w/_w$)$_{final}$ ± SEM	Size (nm) ± SEM	Pdi ± SEM	%Load ± SEM	Entrapped MTO ≥1 year, 4°C ± SEM	Size (nm) ≥1 year, 4°C ± SEM
Non-enriched	0.045	0.075 ± 0.014	0.068 ± 0.005	86 ± 0.7	0.06 ± 0.00	75 ± 4.8	84 ± 4.3	91 ± 1.0
C_8-GluCer	0.045	0.078 ± 0.014	0.070 ± 0.004	84 ± 0.7	0.08 ± 0.01	96 ± 3.3	94 ± 5.7	87 ± 1.3
C_8-GalCer	0.045	0.088 ± 0.016	0.073 ± 0.003	84 ± 1.5	0.07 ± 0.01	93 ± 4.2	81 ± 5.7	85 ± 1.2

More than 3 independent batches were formulated for each formulation and each measurement was performed in triplicate

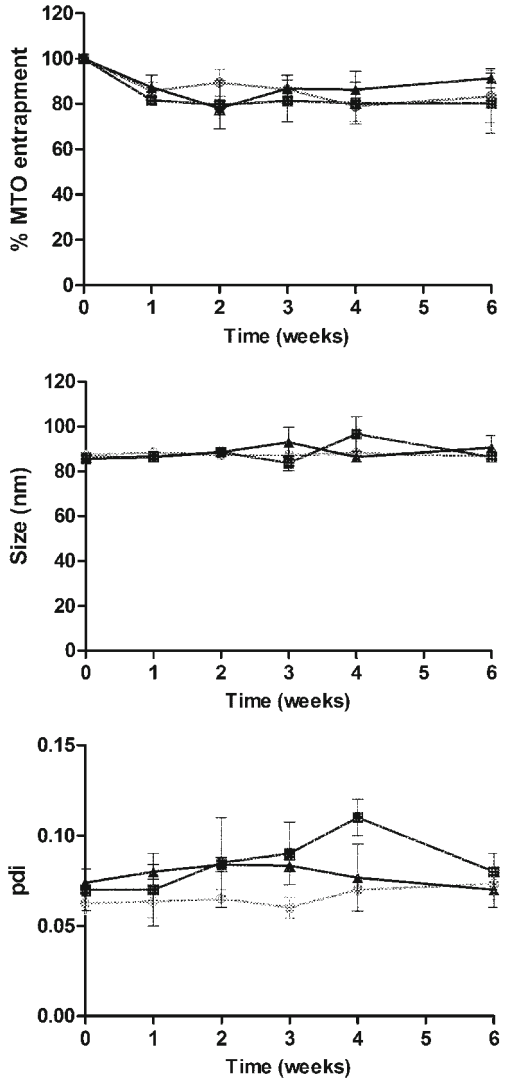

Fig. 1 Stability at 4°C during 6 weeks of different MTO-containing SCS-enriched liposomes (non-enriched (●), C_8-GluCer (■) and C_8-GalCer-MTOL (▲)). Liposomal drug content, size and pdi were analyzed. Three independent experiments were performed testing at least three independent batches and values represent the mean ± SEM.

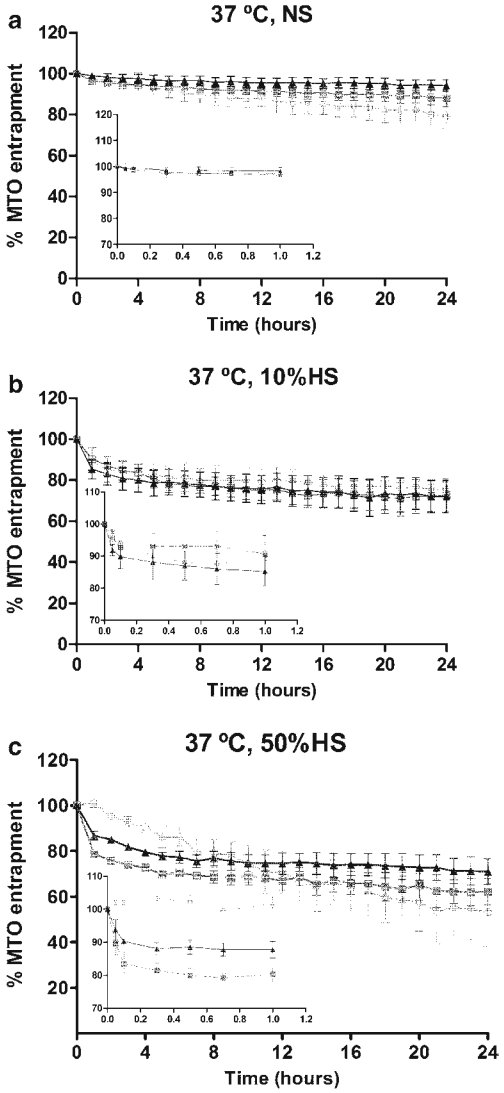

Fig. 2 Stability at 37°C in absence (**a**) and presence of 10% (**b**) or 50% (**c**) human serum of non-enriched MTOL (●) C_8-GluCer-MTOL (■) and C_8-GalCer-MTOL (▲) for 24 h. Graph inserts represent MTO release within the first hour. At least three independent batches from each formulation were tested and values represent the mean ± SEM.

Drug uptake enhancement by SCS was much less pronounced in non-tumor cells. In human endothelial cells (HUVEC) no significant differences were distinguished between MTOL and C_8-GluCer or C_8-GalCer-MTOL treatments neither after 4 or 24 h ($p>0.05$). Fibroblast (3T3) had much lower MTO uptake compared to tumor cells. C_8-GluCer-MTOL induced higher MTO uptake ($p<0.01$) than MTOL after 24 h, whereas C_8-GalCer-MTOL treatment did not yield differences in drug uptake compared to MTOL.

Intracellular Fate of Nanoliposomes, SCS and MTO

To study the intracellular fate of MTO, SCS and the liposomal nanocarrier, confocal microscopy was performed 2 h after incubation of cells with MTOL containing NBD-GalCer and/or Rho-PE and by using the intrinsic fluorescent nature of the drug molecule. Fluorescently labelled NBD-GalCer was observed to transfer from the liposomal to the cell membrane (Fig. 6a). MTO from SCS-MTOL was internalized and localized mainly in the nucleus. C_8-GluCer or C_8-GalCer-MTOL delivered high intracellular MTO levels compared to MTOL, which did not show detectable MTO uptake after 2 h incubation, confirming earlier flow cytometry and cytotoxicity data. Possible liposome uptake was studied by labeling the liposomal bilayer with Rhod-PE, a stable bilayer marker. Liposome uptake by the tumor cells did not occur as evidenced by the red fluorescence from Rho-labelled liposomes surrounding the cells in the medium, which was neither associated with the cells nor internalized, in contrast to the NBD-GalCer and MTO.

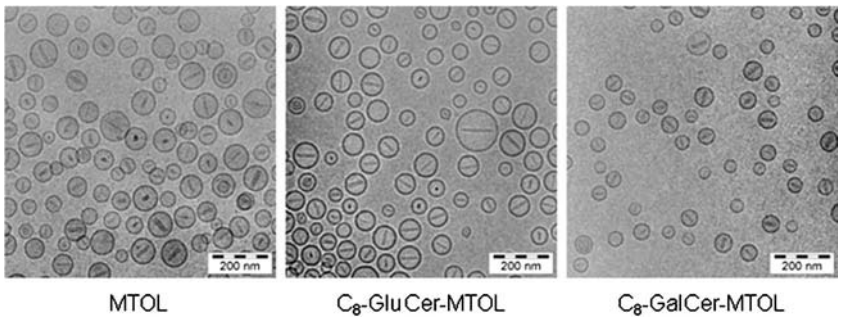

Fig. 3 Cryo-TEM images of liposomes with or without SCS. A clear MTO precipitate is visible inside liposomes. SCS-MTOL are uniform in size and shape and comparable to non-enriched-MTOL. The bar represents 200 nm. A 12500× magnification was used.

In addition, pre-treating SKBR3 breast carcinoma cells with empty SCS enriched-liposomes followed by a washing and subsequent incubation with non-enriched MTOL demonstrated increased MTO uptake that they did not display upon single treatment (Fig 6a), suggesting that SCS transfer occurs independent on the drug influx (Fig. 6b).

Intratumoral Fate of MTO

Intratumoral MTO delivery from SCS-MTOL was compared to MTOL to study whether presence of SCS in the formulation affects MTO accumulation in the tumor and the intratumoral fate of the liposomes. MCF-7 tumor-bearing mice were treated intravenously with MTOL, SCS-MTOL or free MTO at 5 mg*kg^{-1} after which tumors were isolated 24 h after liposome administration and analyzed for intratumoral presence of liposomal drug. Slices of snap-frozen tumor tissue were prepared and analyzed directly for MTO fluorescence by confocal microscopy. Subsequently slices were fixed and stained for tumor vessels and macrophages and imaged to study possible localization of MTO in these different cell types.

For all MTOL formulations, non-enriched, C_8-GluCer and C_8-GalCer (Fig. 7a), rather similar heterogeneous drug distribution patterns within the tumor were observed. Confocal micrographs showed that liposomal-MTO delivery clearly correlated with CD31-positive tumor vessels, mainly in the tumor periphery (Fig. 7a). Further, nuclear uptake of MTO was observed in tumor tissue, surrounding the leaky tumor vessels. Occasionally, more centrally located regions with MTO fluorescence were observed. For free MTO treatment only marginal MTO fluorescence was observed in the tumor periphery suggesting an important improvement in tumor drug delivery by liposomal formulation. Co-localization of liposomal MTO with CD11b positive cells (Fig. 7b), tumor associated macrophages (TAM) and in the stroma was observed to a minor extent and mainly in the better vascularized tumor periphery for all liposome-based treatments. CD11b positive cells were observed throughout the tumor in locations devoid of MTO fluorescence.

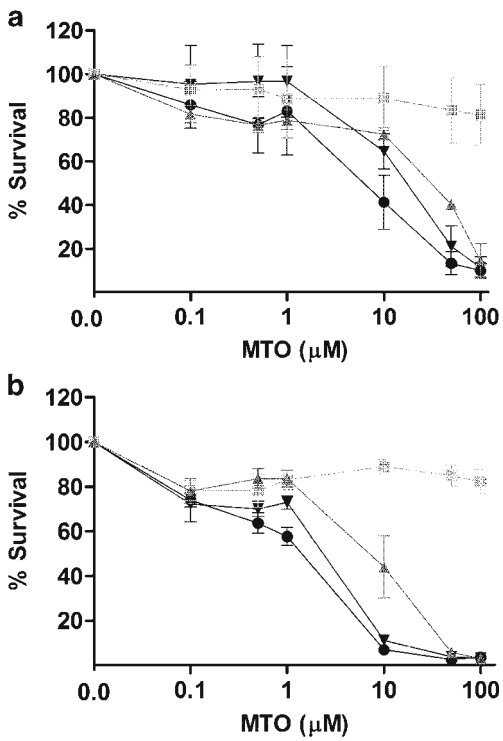

Fig. 4 *In vitro* drug efficacy toward breast carcinoma tumor cells, MCF-7 and SKBR-3. Cells were treated with Free MTO (●) non-enriched-MTOL (■) C_8-GluCer-MTOL (▲) and C_8-GalCer-MTOL (▼) for 24 h at 37°C. Cell survival was quantified by colorimetric SRB assay. Values represent the mean ± SEM of at least 3 independent experiments, testing at least three independent batches.

Table II *In vitro* cytotoxicity (IC_{50}, μM) of Free MTO, non-enriched and SCS-MTOL in breast carcinoma cell lines

	MTO	MTOL	C_8-GluCer-MTOL	C_8-GalCer-MTOL
Tumor cells				
MCF-7	8.3 ± 6.3*	>200	16.1 ± 3.6*	14.8 ± 5.6*
SKBR3	1.0 ± 0.2*	>200	6.2 ± 2.5*	1.6 ± 0.3*

At least three independent experiments were performed and values represent the mean ± SEM

*$P < 0.05$ vs Non enriched MTO-L

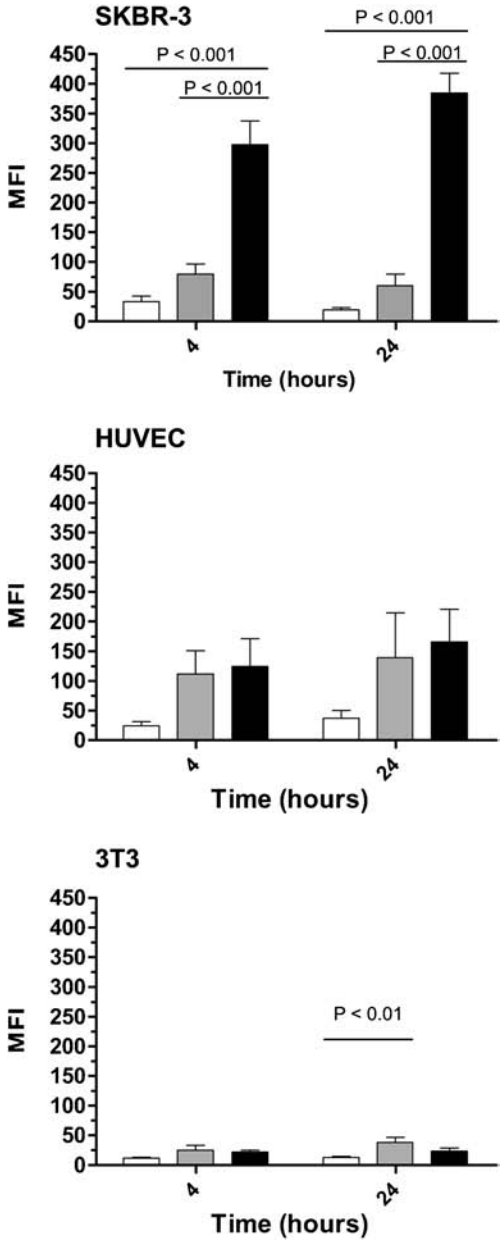

Fig. 5 Intracellular MTO uptake after treatment with MTO liposomes (10 μM), quantified by flow cytometry in breast carcinoma cells (SKBR3) and non-tumor endothelial cells (HUVEC) and fibroblasts (3T3). MTO was formulated in non-enriched liposomes (*open*), C_8-GluCer-MTOL (*grey*) and C_8-GalCer-MTOL (*black*). At least three independent experiments were performed and values represent the mean ± SEM.

DISCUSSION

Although MTO has been developed as a less toxic alternative for anthracycline chemotherapy, side effects are not absent and remain an important reason for inadequate dosing for tumor treatment. Liposomal encapsulation is a clinically proven strategy to further decrease toxic side effects of chemotherapeutic drugs [14] and is successfully applied in this study. Whereas liposomal encapsulation positively affects drug toxicity, it is less beneficial for effective delivery of bioavailable drug into tumor cells [19, 20, 22]. To overcome the latter obstacle we applied a novel drug delivery strategy targeting tumor cell membrane composition by insertion of short-chain sphingolipids (SCS) to improve chemotherapeutic drug uptake [24–28]. To optimally combine both strategies to the benefit of MTO chemotherapy, we developed novel liposomal MTO formulations carrying the drug inside and the SCS in their bilayer. Homogeneous and stable formulations of SCS-MTOL were prepared with small size (<100 nm) and high MTO content, which upon remote loading was found in nanocrystalline form intraliposomally. SCS, upon their transfer to tumor cell membranes, strongly improved the drug delivery capacity of MTOL as was observed by live cell confocal imaging and flow cytometry, resulting in strongly improved *in vitro* anti-tumor activity toward human breast carcinoma. Remarkably, this drug delivery process displayed selectivity for tumor cells over normal cells. Both endothelial cells and especially fibroblasts appeared much less affected upon treatments with this novel SCS-MTOL. On-going studies focus on the underlying mechanism of this cell type specificity for SCS-mediated tumor cell membrane permeabilization. Liposomal formulations were able to deliver detectable drug quantities to orthotopic human breast carcinoma tumors, in contrast to free MTO treatment. SCS modification of the MTOL did not notably affect intratumoral distribution patterns of MTO. This combined with the demonstrated improvements that SCS add to the intracellular drug delivery process make us conclude that these novel SCS-MTOL formulations hold promise for further improvement in MTO cancer chemotherapy.

Remote loading of chemotherapeutic drugs into small unilamellar vesicles (SUVs) offers advantages of high entrapment levels and safety in the preparation procedure and has been applied for multiple anti-cancer drugs [30]. Such loading procedure requires a pH or ammonium sulphate gradient and both were applied for MTO encapsulation. The pH gradient method using intraliposomal citrate buffer of pH 4 yielded unstable aggregating particles with low drug entrapment. The ammonium sulphate method however yielded higher drug entrapment levels observed as a precipitate in the liposome core and did not induce aggregation. Liposomes containing MTO were uniformly round shaped independently on the presence of SCS in the liposomal bilayer. Interestingly, these findings differ from those we obtained with SCS-enriched liposomes loaded with Doxorubicin, on which we previously reported [27]. These SCS-Doxorubicin liposomes were to some extent rod-shaped when co-formulated with SCS, while non-enriched liposomes were uniformly round-shaped [27]. For both amphiphilic drugs, the presence of SCS improved drug-loading efficiency in relation to non-enriched liposomes. However, the mechanism to form the intraliposomal precipitates differs. In the liposomal core,

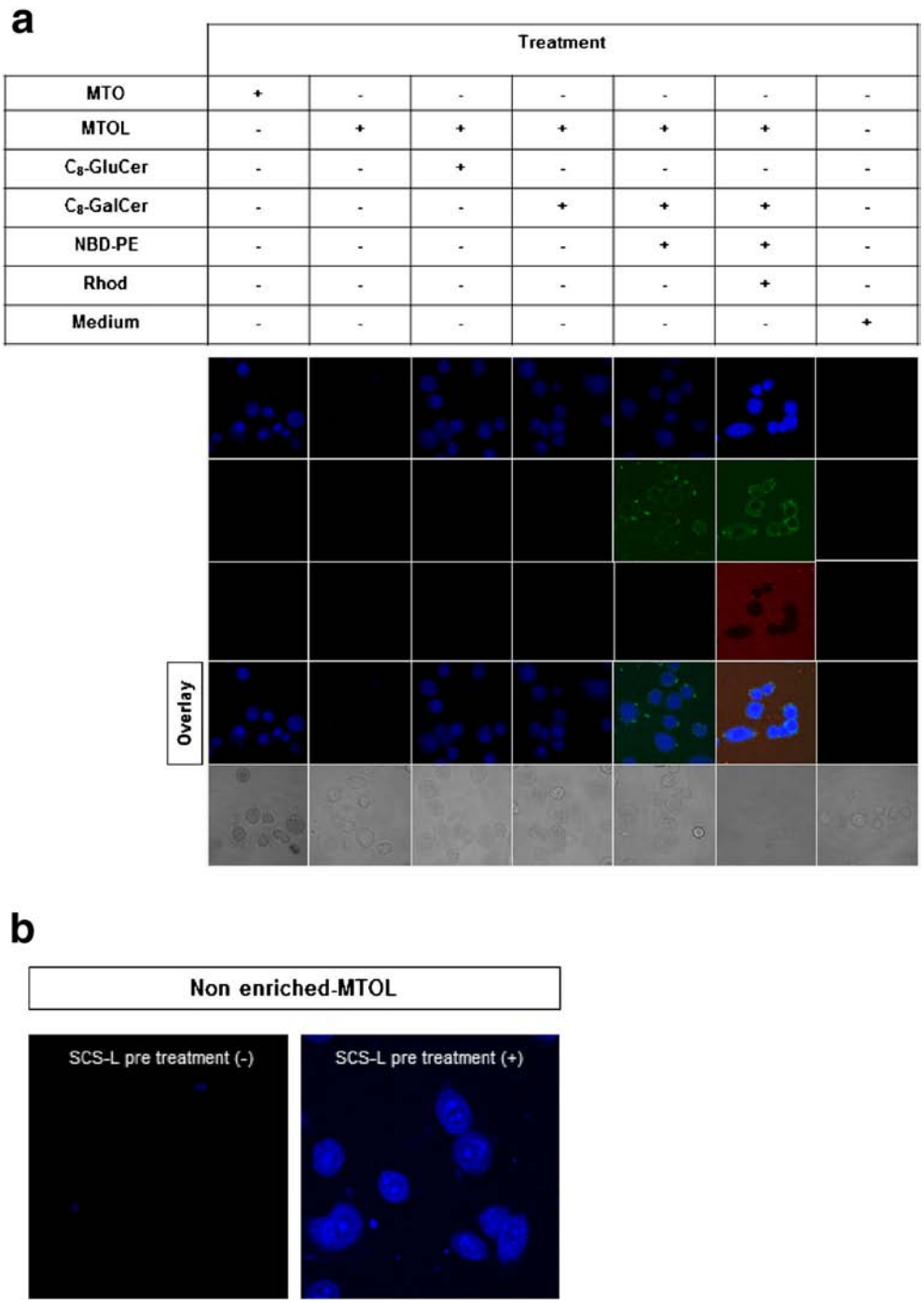

Fig. 6 Cellular localization of SCS and MTO studied by confocal microscopy (**a**). SKBR3 breast carcinoma cells were treated for 2 h at 37°C with NBD labeled-GalCer (5 μM) liposomes containing MTO (10 μM), the green fluorescent labeled-GalCer was imaged separately from MTO. The SCS accumulates in the plasma membrane and MTO accumulates in the nucleus and cytoplasm. Intracellular-localization of Rhodamine labeled liposomes (*red*) wasn't seen. Pre-incubating cells with C_8-GalCer liposomes not containing MTO for 1 h followed by washing and treatment with MTOL (10 μM), resulted in intracellular drug levels comparable to direct treatment with C_8-GalCer-MTOL (10 μM) (**b**).

MTO and Doxorubicin associate to sulphate anions by double and single NH-groups, respectively. Additionally, Doxorubicin is able to self-stack into fibers through hydrophobic interactions which are bridged by the sulphate anions [38], inducing higher levels of intraliposomal drug, which may deform the liposomes to rod-shaped structures. In fact, optimal drug:lipid ratio for loading of MTO was lower than for Doxorubicin. SCS-enriched MTO liposomes were formulated with 10 mol% of C_8-GluCer or C_8-GalCer as SCS-enriched Doxorubicin liposomes, due to similarity on their drug loading method and liposomal lipid composition. Different amounts of SCS have been tested in the enriched formulations. For C_8-GluCer enriched liposomes containing Doxorubicin, 5, 10 and 15 mol% of lipid were tested demonstrating that 10 mol% SCS co-inserted in the liposomal bilayer consisted of the optimal amount in terms of intracellular drug uptake enhancement [24] with 15 mol% not giving any additional effect. Additionally, Pedrosa et al., 2013 confirmed

that 10 mol% C_8-GalCer represented the optimal amount to enrich Doxorubicin-liposomes achieving maximal intracellular drug uptake [27].

For MTO-loading a D:PL ratio of 0.07 (*w*/*w*) was determined optimal for non-enriched and SCS-enriched-MTOL, resulting in maximal drug loading efficiency. SCS-enriched nanoliposomes reached a higher MTO loading efficiency close to 100% against 75% for non-enriched nanoliposomes. Likely, the presence of SCS, C_8-GluCer and C_8-GalCer in the liposomal bilayer helped to improve MTO entrapment. The exposed hydroxyl groups of the sugar moiety of the hydrophilic SCS head group may promote MTO interaction through hydrogen binding thereby increasing the loading efficiency [39].

Concerning stability (Figs. 1 and 2), both MTOL and SCS-MTOL had similarly low levels of MTO release, presenting characteristics of an optimal formulation from a pharmaceutical point of view: maximum drug content and high stability together with maintenance of physical properties, such as size <100 nm and pdi <0.1. The initial drug release, which was observed both during storage and in the first hour at 37°C of incubation, can be explained by the release of MTO associated to the phospholipid bilayer. Considering that HSPC is neutral and PEG-DSPE is negatively charged and that MTO has a tendency to associate with negatively charged lipids at a pH between 5 and 8 could explain its presence in and drug release from the liposomal membrane at 37°C for all liposomal formulations, especially in the presence of serum. In the

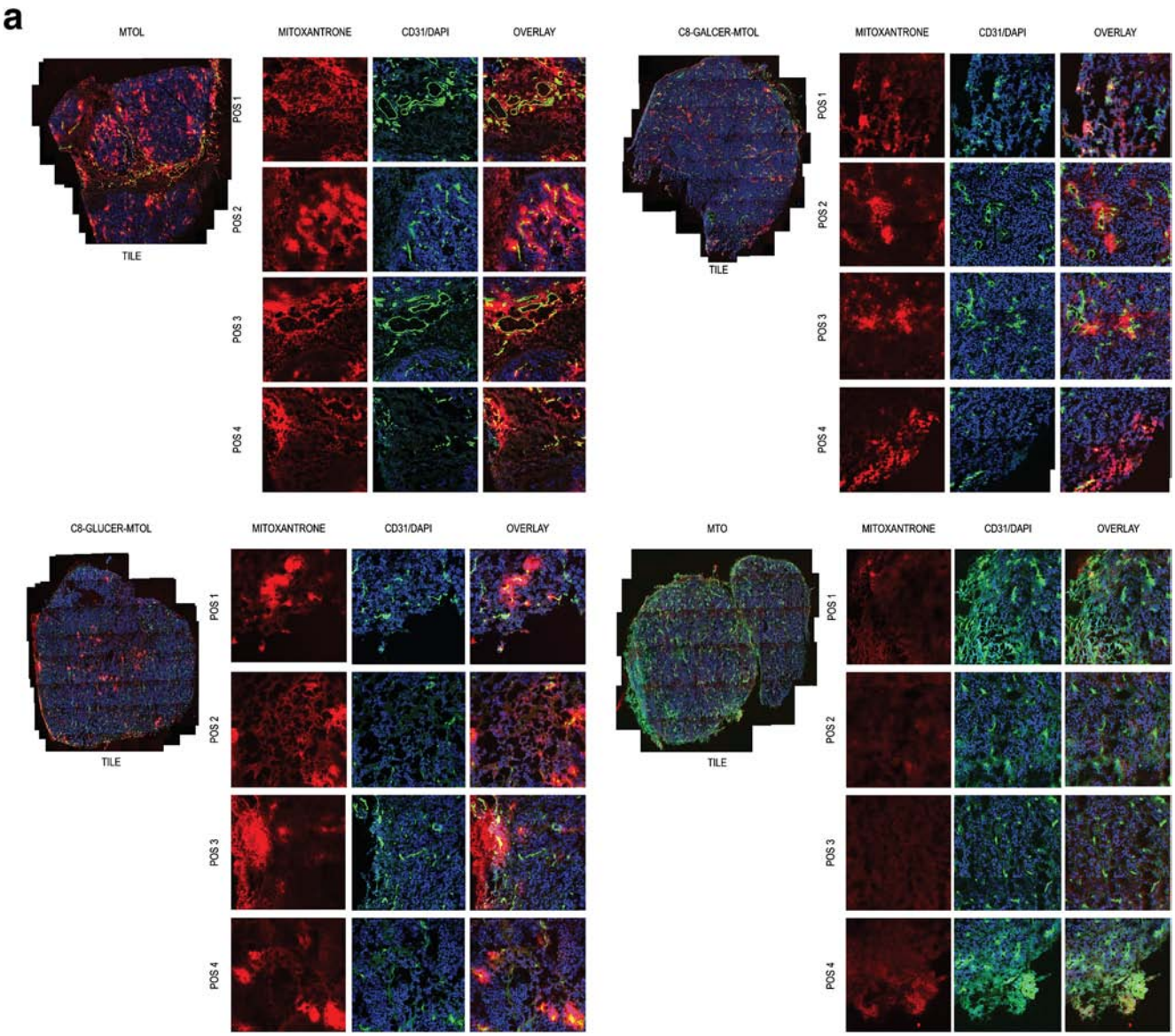

Fig. 7 Fluorescence micrographs of orthotopic MCF-7 breast carcinoma frozen sections, obtained from NMRI-nude female mice 24 h after i.v injection of MTO (5 mgKg-1) in form of standard MTOL and SCS-MTOL (C8-GluCer and C8-GalCer). After MTO imaging, frozen sections were stained for (**a**) anti-CD31, macrophages and (**b**) anti-CD11b antibody (vessels).

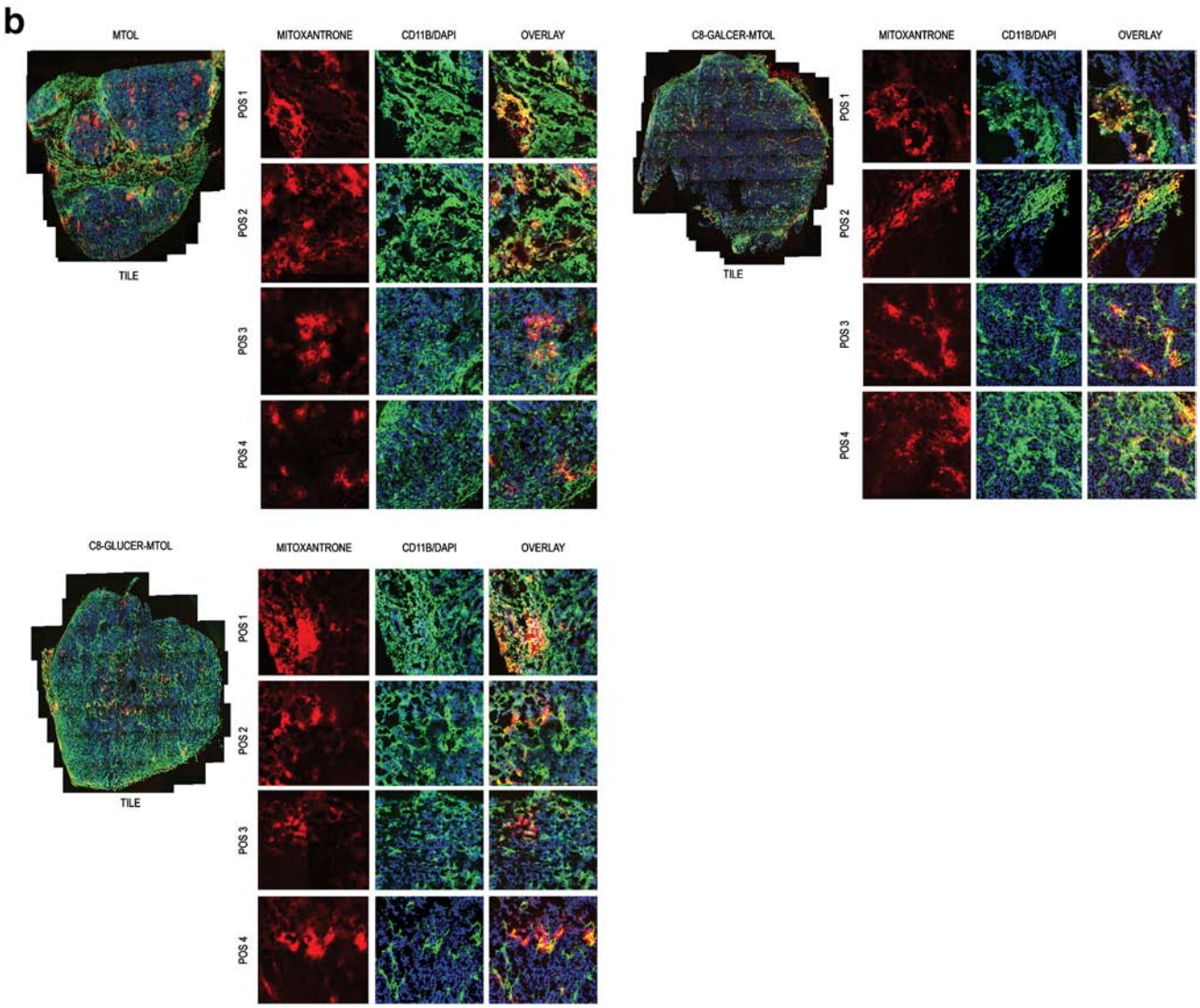

Fig. 7 (continued)

presence of 50% human serum, non-enriched liposomes continuously released MTO, indicating a contribution from the intraliposomal MTO pool. Instead, SCS-MTOL initially released MTO, but after that retained their intraliposomal MTO content. Therefore it can be assumed that SCS when inserted in the liposomal bilayer, together with improving drug loading efficiency also contributed to the stability profile of the nanoliposomes, improving MTO retention at high density serum better than non-enriched-MTOL.

Although SCS did not affect MTO release, they synergistically acted with liposomal MTO to improve its intracellular delivery and efficacy towards breast carcinoma cells. 24 h incubation of tumor cells with SCS-MTOL markedly increased cytotoxicity compared to non-enriched MTOL. IC_{50} values for free MTO and SCS-enriched liposomes containing MTO were comparable in SKBR3 and MCF-7 breast cancer cells (Fig. 4 and Table II). Considering that SCS-enriched liposomes are stable in presence of 10% serum - mimicking *in vitro* conditions (Fig. 2b), cytotoxicity studies performed in 10% serum, demonstrate that SCS enriched liposomes enhance intracellular drug uptake reaching an efficacy comparable to free drug treatment, by other means then leakage from the liposomes. Yet, standard liposomes containing MTO presented similarly high stability at 10% serum, but were much less efficacious due to lack in drug bioavailability. Previous studies demonstrated the potency of SCS as drug uptake enhancers for Doxorubicin when using nanoscale liposomal drug delivery systems [24, 26–28]. Here, we confirm this for MTO. Remarkably, SCS mediated drug uptake displayed a clear selectivity for tumor cells when compared to normal cells, such as endothelial cells and fibroblasts that were much less affected by SCS-MTOL. Furthermore, after 4 h the

highest drug levels were reached and maintained to 24 h demonstrating an early maximized effect of the enhancing drug uptake properties of SCS (Fig. 5). When comparing C_8-GluCer and C_8-GalCer we learned that different short-chain glycoceramides can affect cellular drug uptake differently in the same tumor cell line. C_8-GluCer and C_8-GalCer differences on the equatorial and axial, respectively, 1-hydroxyl group position in the molecular structure of the lipid headgroup might differentially affect the lipid rearrangement/packing of the cell membrane and thereby influence drug membrane traversal. C_8-GalCer-MTOL caused much higher MTO uptake in SKBR3 cells than C_8-GluCer-MTOL as quantified by flow cytometry subsequently causing more toxicity towards this cell line. These observations are well in line with previous findings with SCS-liposomal Doxorubicin [27]. Also in that study, SCS provided specificity of Doxorubicin delivery to tumor cell membranes in comparison to normal cells and more subtly also showed that different SCS displayed preferential activity in some tumor cell lines compared to others. These observations suggest that responsiveness to SCS mediated drug delivery is not only (tumor) cell type specific, but is also dependent on the nature of the SCS. Optimal combinations of drugs and SCS may be available for particular tumor cell types. Such combinations can be obtained by extensive screening of lipids and drugs that will be part of future studies in which also the importance of the lipid composition of the receiving cell membrane will be investigated. Figure 8 illustrates the proposed mechanism of action for SCS as intracellular drug uptake enhancers.

Previous studies already indicated SCS transfer to the cell membrane precedes Doxorubicin transfer and cellular influx [27, 28]. As shown by confocal microscopy (Fig. 6), MTO is transported across the cell membrane and through the cytoplasm reaching the nucleus where it is retained and active [10, 40]. Upon labelling liposomes with Rhodamine-PE, a stable bilayer marker, we could prove that liposomes are not taken up by the cells. Yet, SCS are transferred from the liposomal bilayer to the cell membrane, via a process which is not related to cellular nanoparticle uptake. Interestingly SCS delivered to tumor cell membranes by non-drug containing liposomes could similarly promote MTO uptake from non SCS-containing MTOL (Fig. 6b) indicating that SCS transfer and MTO uptake act independent of the liposomal carrier and synergize at the cell membrane level.

Although the *in vitro* drug delivery route for the novel SCS-MTOL could be elucidated, the *in vivo* situation is much more complex with the presence of various tumor physiological barriers and multiple cell types within a tumor. To gain further understanding of *in vivo* tumor drug delivery we investigated the intratumoral fate of MTO when administered i.v as MTOL, C_8-GluCer or C_8-GalCer-MTOL or free drug. Detectable MTO levels, 24 h after i.v. administration were only observed upon treatment with liposomal formulations and not upon free MTO administration demonstrating that nanoparticle mediated drug delivery can help to extend tumor drug exposure. Low tumor drug levels after free MTO treatment correlate to the large volume of distribution of the free drug and its rapid clearance from circulation [41]. Liposomal encapsulation is known to extend drug circulation time [17] and this in combination with immature, more leaky tumor vasculature can lead to liposome extravasation and interstitial accumulation of both carrier and drug [42, 43]. Here, all liposomal formulations delivered their MTO content mainly perivascularly in a rather heterogeneous manner throughout the tumor correlating with the tumor vascular make-up. Certainly not all vessels were characterized by MTO presence suggesting that not all tumor vessels allow liposome extravasation and subsequent drug delivery. Tumor vasculature is very heterogeneous and permeability of a specific tumor vessel does not only depend on perfusion of the vessel, but also on the intrinsic profile of the endothelial lining and the surrounding microenvironment [44]. Therefore, strategies to induce increased vascular permeability using for instance biological vascular modifiers as TNF-α or physical treatments with for instance hyperthermia may further improve interstitial nanoparticle-mediated drug delivery [19, 20, 45].

From our observations in an orthotopic human breast carcinoma tumor, in presence or absence of SCS, fluorescent MTO is observed intracellularly as well as extracellularly. Upon interstitial localization drug release may involve gradual release from the liposomes and subsequent cellular uptake as

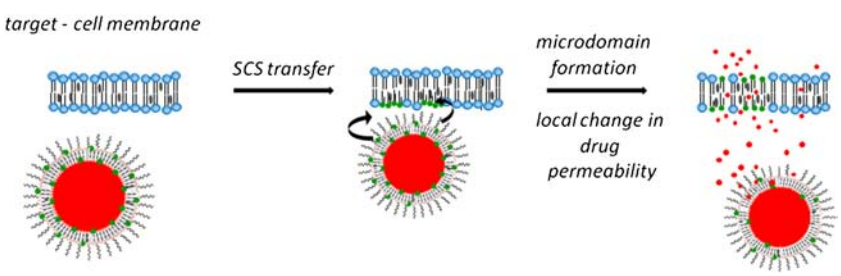

Fig. 8 Illustration of SCS mechanism of action. SCS (*green*) in the liposome bilayer are transferred to tumor cell membrane creating enhanced permeabilized specific areas improving intracellular drug (*red*) uptake. Drug influx occurs at a later stage and is transferred from the liposome core to the independently on previously lipid transfer.

in the in vitro situation. Tumor tissue is, in addition to tumor cells, composed of stromal cells, which may also take up the drug. Importantly, SCS in vitro clearly displayed a preference to enhance MTO delivery into tumor cells and to a much lesser extent in fibroblasts and endothelial cells (Fig. 5).

Whereas some studies concluded a role of tumor associated macrophages (TAM) in drug release from liposomes [46], others have described that tumor uptake of liposomal drugs does not correlate with the presence of TAM [47, 48]. It was proposed that the respective improvement in drug delivery may be related to an alternative TAM-mediated processes that increases tumor vasculature permeability and liposome localization in TAM-rich areas. These findings are in accordance with Banciu et al. [48] who reported that the anti tumor effect of liposomal Doxorubicin (Doxil) does not depend on the presence of functional TAM in tumors. In the present study, MCF-7 tumors had a considerable TAM content localized in particular zones in the tumor. Although liposomal MTO was also delivered in these tumor regions, drug delivery was not solely restricted to macrophage enriched areas, but also occurred in different regions lacking TAM presence. As no major differences were found in tumor drug delivery patterns between non-enriched MTOL and SCS-MTOL it is likely that SCS do not promote co-localization of the SCS-MTOL with macrophages.

CONCLUSION

In conclusion, a novel nanoliposomal formulation of MTO with bilayer inserted SCS has been developed that displayed tumor cell specific, enhanced drug delivery. Whereas liposomal formulation improved tumor drug delivery compared to free MTO, SCS improved cellular MTO uptake preferentially in tumor cells. This new concept of drug delivery by targeting tumor cell membrane composition, modulating its permeability constitutes a promising direction to improve MTO chemotherapy efficacy.

ACKNOWLEDGEMENTS AND DISCLOSURES

This work was financed by the Dutch Cancer Society. The authors thank Thomas Soullié for technical assistance with various aspects of histology and data processing and Sabine Barnert for performing cryo-TEM analyses.

REFERENCES

1. Dunn CJ, Goa KL. Mitoxantrone: a review of its pharmacological properties and use in acute nonlymphoblastic leukaemia. Drugs Aging. 1996;9(2):122–47.
2. White RJ, Durr FE. Development of mitoxantrone. Investig New Drugs. 1985;3(2):85–93.
3. Koutinos G, Stathopoulos GP, Dontas I, *et al.* The effect of doxorubicin and its analogue mitoxantrone on cardiac muscle and on serum lipids: an experimental study. Anticancer Res. 2002;22(2A):815–20.
4. Chungun A, Uchide T, Tsurimaki C, *et al.* Mechanisms responsible for reduced cardiotoxicity of mitoxantrone compared to doxorubicin examined in isolated guinea-pig heart preparations. J Vet Med Sci. 2008;70:255–64.
5. Murray TJ. The cardiac effects of mitoxantrone: do the benefits in multiple sclerosis outweigh the risks? Expert Opin Drug Saf. 2006;5(2):265–74.
6. Cristofanilli M, Holmes F, Esparza L, *et al.* Phase I/II trial of high dose mitoxantrone in metastatic breast cancer: the M.D. Anderson Cancer Center experience. Breast Cancer Res Treat. 1999;54(3):225–33.
7. Pusztai L, Holmes FA, Fraschini G, Hortobagyi GN. Phase II study of mitoxantrone by 14-day continuous infusion with granulocyte colony-stimulating factor (GCSF) support in patients with metastatic breast cancer and limited prior therapy. Cancer Chemother Pharmacol. 1999;43(1):86–91.
8. Cook AM, Chambers EJ, Rees GJG. Comparison of mitozantrone and epirubicin in advanced breast cancer. Clin Oncol. 1996;8:363–6.
9. Faulds D, Balfour J, Chrisp C, Langtry D. Mitoxantrone. A review of its pharmacodynamic and pharmacokinetic properties, and therapeutic potential in the chemotherapy of cancer. Drugs. 1991;41(3):400–49.
10. Fox EJ. Mechanism of action of mitoxantrone. Neurology. 2004;63(12 suppl 6):S15–8.
11. Feofanov A, Sharonov S, Kudelina I, Fleury F, Nabiev I. Localization and molecular interactions of mitoxantrone within living K562 cells as probed by confocal spectral imaging analysis. Biophys J. 1997;73(6):3317–27.
12. Hajihassan Z, Rabbani-Chadegani A. Studies on the binding affinity of anticancer drug mitoxantrone to chromatin, DNA and histone proteins. J Biomed Sci. 2009;16(31).
13. van Dalen EC, van der Pal HJH, Bakker PJM, Caron HN, Kremer LCM. Cumulative incidence and risk factors of mitoxantrone-induced cardiotoxicity in children: a systematic review. Eur J Cancer. 2004;40(5):643–52.
14. Allen TM, Cullis PR. Liposomal drug delivery systems: from concept to clinical applications. Adv Drug Deliv Rev. 2013;65(1):36–48.
15. Paliwal SR, Paliwal R, Agrawal GP, Vyas SP. Liposomal nanomedicine for breast cancer therapy. Nanomedicine (London). 2011;6(6):1085–100.
16. Koning GA, Krijger GC. Targeted multifunctional lipid-based nanocarriers for image-guided drug delivery. Anti Cancer Agents Med Chem. 2007;7(4):425–40.
17. Mattheolabakis G, Rigas B, Constantinides PP. Nanodelivery strategies in cancer chemotherapy: biological rationale and pharmaceutical perspectives. Nanomedicine (London). 2012;7(10):1577–90.
18. Deshpande PP, Biswas S, Torchilin VP. Current trends in the use of liposomes for tumor targeting. Nanomedicine (London). 2013;8(9):1509–28.
19. Seynhaeve AL, Dicheva BM, Hoving S, Koning GA, Ten Hagen TL. Intact doxil is taken up intracellularly and released doxorubicin sequesters in the lysosome: evaluated by in vitro/in vivo live cell imaging. J Control Release. 2013;172(1):330–40.
20. Seynhaeve ALB, Hoving S, Schipper D, *et al.* Tumor necrosis factor Î ± mediates homogeneous distribution of liposomes in murine melanoma that contributes to a better tumor response. Cancer Res. 2007;67(19):9455–62.
21. O'Brien MER, Wigler N, Inbar M, *et al.* Reduced cardiotoxicity and comparable efficacy in a phase III trial of pegylated liposomal doxorubicin HCl (CAELYXâ"¢/DoxilÂ®) versus conventional doxorubicin for first-line treatment of metastatic breast cancer. Ann Oncol. 2004;15(3):440–9.

22. Laginha KM, Verwoert S, Charrois GJR, Allen TM. Determination of doxorubicin levels in whole tumor and tumor nuclei in murine breast cancer tumors. Clin Cancer Res. 2005;11(19 Pt1):6944–9.
23. Visani G, Isidori A. Doxorubicin variants for hematological malignancies. Nanomedicine (London). 2011;6(2):303–6.
24. van Lummel M, van Blitterswijk WJ, Vink SR, 1, *et al.* Enriching lipid nanovesicles with short-chain glucosylceramide improves doxorubicin delivery and efficacy in solid tumors. FASEB J. 2009;25:280–9.
25. Veldman RJ, Zerp S, van Blitterswijk WJ, Verheij M. N-hexanoyl-sphingomyelin potentiates in vitro doxorubicin cytotoxicity by enhancing its cellular influx. Br J Cancer. 2004;90(4):917–25.
26. Veldman RJ, Zerp S, van Blitterswijk WJ, *et al.* Coformulated N-octanoyl-glucosylceramide improves cellular delivery and cytotoxicity of liposomal doxorubicin. J Pharmacol Exp Ther. 2005;315(2):704–10.
27. Pedrosa LRC, Hell A, Suss R, *et al.* Improving intracellular doxorubicin delivery through nanoliposomes equipped with selective tumor cell membrane permeabilizing short-chain sphingolipids. Pharm Res. 2013;30(7):1883–95.
28. van Hell AJ, Melo MN, van Blitterswijk WJ, *et al.* Defined lipid analogues induce transient channels to facilitate drug-membrane traversal and circumvent cancer therapy resistance. Sci Rep. 2013;3:1949.
29. Siskind LJ, Fluss S, Bui M, Colombini M. Sphingosine forms channels in membranes that differ greatly from those formed by ceramide. J Bioenerg Biomembr. 2005;37(4):227–36.
30. Haran G, Cohen R, Bar LK, Barenholz Y. Transmembrane ammonium sulfate gradients in liposomes produce efficient and stable entrapment of amphipathic weak bases. Biochim Biophys Acta. 1993;1151(2):201–15.
31. Pinto AC, Moreira JN, Simões S. Liposomal imatinib-mitoxantrone combination: formulation development and therapeutic evaluation in an animal model of prostate cancer. Prostate. 2011;71(1):81–90.
32. Li C, Cui J, Wang C, *et al.* Encapsulation of mitoxantrone into pegylated SUVs enhances its antineoplastic efficacy. Eur J Pharm Biopharm. 2008;70(2):657–65.
33. Lim HJ, Masin D, Madden TD, Bally MB. Influence of drug release characteristics on the therapeutic activity of liposomal mitoxantrone. J Pharmacol Exp Ther. 1997;281(1):566–73.
34. Rouser G, Fkeischer S, Yamamoto A. Two dimensional thin layer chromatographic separation of polar lipids and determination of phospholipids by phosphorus analysis of spots. Lipids. 1970;5(5):494–6.
35. Jaffe EA, Nachman RL, Becker CG, Minick CR. Culture of human endothelial cells derived from umbilical veins. Identification by morphologic and immunologic criteria. J Clin Invest. 1973;52(11):2745–56.
36. Skehan P, Storeng R, Scudiero D, *et al.* New colorimetric cytotoxicity assay for anticancer-drug screening. J Natl Cancer Inst. 1990;82(13):1107–12.
37. Li L, ten Hagen TLM, Schipper D, 2, *et al.* Triggered content release from optimized stealth thermosensitive liposomes using mild hyperthermia. J Control Release. 2010;143:274–9.
38. Li X, Hirsh DJ, Cabral-Lilly D, 1, *et al.* Doxorubicin physical state in solution and inside liposomes loaded via a pH gradient. Biochim Biophys Acta. 1998;1415:23–40.
39. Law SL, Chang P, Lin CH. Characteristics of mitoxantrone loading on liposomes. Int J Pharm. 1991;70:1–7.
40. Durr FE, Wallace RE, Citarella RV. Molecular and biochemical pharmacology of mitoxantrone. Cancer Treat Rev. 1983;10(Suppl B):3–11.
41. Orthmann A, Zeisig R, Suss R, *et al.* Treatment of experimental brain metastasis with MTO-liposomes: impact of fluidity and LRP-targeting on the therapeutic result. Pharm Res. 2012;29(7):1949–59.
42. Maeda H, Nakamura H, Fang J. The EPR effect for macromolecular drug delivery to solid tumors: improvement of tumor uptake, lowering of systemic toxicity, and distinct tumor imaging in vivo. Adv Drug Deliv Rev. 2013;65(1):71–9.
43. Yuan F, Leunig M, Huang SK, Berk DA, Papahadjopoulos D, Jain RK. Microvascular permeability and interstitial penetration of sterically stabilized (stealth) liposomes in a human tumor xenograft. Cancer Res. 1994;54(13):3352–6.
44. Nakasone ES, Askautrud HA, Kees T, *et al.* Imaging tumor-stroma interactions during chemotherapy reveals contributions of the microenvironment to resistance. Cancer Cell. 2012;21(4):488–503.
45. Li L, ten Hagen TLM, Schipper D, *et al.* Improved intratumoral nanoparticle extravasation and penetration by mild hyperthermia. J Control Release. 2013;167(2):130–7.
46. Storm G, Steerenberg PA, Emmen F, van Borssum WM, Crommelin DJ. Release of doxorubicin from peritoneal macrophages exposed in vivo to doxorubicin-containing liposomes. Biochim Biophys Acta. 1988;965(2–3):136–45.
47. Mayer LD, Dougherty G, Harasym TO, Bally MB. The role of tumor-associated macrophages in the delivery of liposomal doxorubicin to solid murine fibrosarcoma tumors. J Pharmacol Exp Ther. 1997;80(3):1406–14.
48. Banciu M, Schiffelers RM, Storm G. Investigation into the role of tumor-associated macrophages in the antitumor activity of doxil. Pharm Res. 2008;25(8):1948–55.